Production cross section of At radionuclides from ^{7}Li + ^{nat}Pb and ^{9}Be + ^{nat}Tl reactions

Moumita Maiti* and Susanta Lahiri†

Chemical Sciences Division, Saha Institute of Nuclear Physics, 1/AF, Bidhannagar, Kolkata 700064, India

(Received 10 September 2011; revised manuscript received 23 November 2011; published 16 December 2011)

Earlier we reported theoretical studies on the probable production of astatine radionuclides from ^{6,7}Li- and ^{9}Be-induced reactions on natural lead and thallium targets, respectively. The production of astatine radionuclides were investigated experimentally with two heavy-ion-induced reactions: ^{9}Be + ^{nat}Tl and ^{7}Li + ^{nat}Pb. Formation cross sections of the evaporation residues, ^{207,208,209,210}At, produced in the (HI,xn) channel, were measured by the stacked-foil technique followed by off-line γ spectrometry at low incident energies (<50 MeV). Measured excitation functions were interpreted in terms of a compound nuclear reaction mechanism using Weisskopf-Ewing and Hauser-Feshbach models. Measured cross-section values are lower than the respective theoretical predictions.

DOI: 10.1103/PhysRevC.84.067601 PACS number(s): 25.70.Gh, 24.60.Dr

Astatine has become of greater interest due to the potential application of ^{211}At in targeted therapy. Owing to suitable nuclear properties, ^{211}At is promising for treating small tumors. Astatine radionuclides are produced artificially in an accelerator because the element has no naturally occurring isotope. The choice of suitable target-projectile combinations and the knowledge of nuclear reaction data are therefore important in producing the radionuclide of choice. However, experimental cross-section data are scarce.

Usually, astatine radionuclides, $^{207-211}$At, are produced by bombarding α particles on natural bismuth targets [1–4]. Other production methods have included ^{3}He-induced reactions on bismuth targets [5–7] and high-energy proton-induced spallation reactions on heavy targets such as ^{238}U, ^{232}Th, etc. A sufficient amount of $^{207-211}$At radionuclides can also be produced by light heavy-ion-induced reactions, which are not well studied. A few reports have dealt with the heavy-ion-induced production of astatine. The experimental measurement of formation cross sections of $^{208-211}$At produced through ^{7}Li- and ^{6}Li-induced reactions on an enriched ^{208}Pb target were reported in Refs. [8,9]. The production of ^{209,210}At was reported in Refs. [10,11], where ^{7}Li was bombarded on a natural lead target with the objective of studying the chemical separation procedures of astatine from bulk lead. The present authors also used a ^{9}Be beam to produce $^{208-210}$At from ^{nat}Tl target and developed appropriate chemical separation methods for the production of At radionuclides [12]. The encouraging yields of At radionuclides in heavy-ion activation prompted us to make a theoretical investigation into the production possibility of astatine radionuclides through ^{nat}Pb(^{7}Li,xn), ^{nat}Pb(^{6}Li,xn), and ^{nat}Tl(^{9}Be,xn) reactions [13]. This Brief Report presents results on the measurement of the excitation functions of $^{207-210}$At produced in ^{7}Li- and ^{9}Be-induced reactions on natural lead and thallium targets, respectively, and are used to validate our theoretical study [13]. Measured cross-section data were analyzed using two well-established nuclear reaction model codes, ALICE91 [14,15] and PACE4 [16]. Because of the limitation associated with the available accelerator facility, this Brief Report only covers a small incident energy range.

The experimental procedure is described as follows. Natural nonhygroscopic thallium carbonate, Tl_2CO_3, and lead nitrate, $Pb(NO_3)_2$, were used as target materials. Targets of uniform thickness, 1.8 ± 0.1 mg/cm^2 Tl_2CO_3 and 3.0 ± 0.3 mg/cm^2 $Pb(NO_3)_2$, were prepared using a centrifugation technique on aluminum foil backing of thickness 1.5 mg/cm^2. Three such targets were mounted into a target assembly, which was then bombarded by the suitable projectile (e.g., ^{7}Li or ^{9}Be) at the BARC-TIFR Pelletron Accelerator facility in Mumbai, India. The Tl_2CO_3 target stack was irradiated with a 47.6-MeV ^{9}Be beam for 4.75 h, resulting in a total charge of 388 μC. The $Pb(NO_3)_2$ target stack was irradiated with 46-MeV ^{7}Li projectiles for 2.82 h, resulting in a total charge of 1336 μC. The residual products, if any, recoiled in the beam direction and were stopped by the aluminum backing. The large area of the catcher foils ensured the complete collection of recoiled evaporation residues. The beam intensity was measured in each experiment from the total charge collected in an electron-suppressed Faraday cup stationed at the rear of the target assembly.

Irradiated foils were counted at the end of bombardment (EOB) to measure the γ-ray activity of the evaporation residues produced in the respective target matrix using a high-purity germanium detector of 2.13-keV resolution at 1332 keV coupled with a PC-based multichannel analyzer. Each foil was counted in a regular time interval until the complete decay of the residues. Use of centrifuged targets on aluminum backing prevented the separate measurement of the recoiled activity induced in the aluminum foils. However, in the present case, recoiled activity in the backing, if any, is expected to be negligible with the low projectile energy used in this experiment.

The beam-energy degradation in the target and the catcher foils was calculated using the Stopping and Range of Ions in Matter (SRIM) code [17]. The projectile energy at the target is the average of incident and outgoing beam energy. Energy loss was about 2% in the thallium carbonate and lead nitrate targets. Product yields of the evaporation residues in each foil were calculated from the background-subtracted peak

*moumita.maiti@saha.ac.in
†susanta.lahiri@saha.ac.in

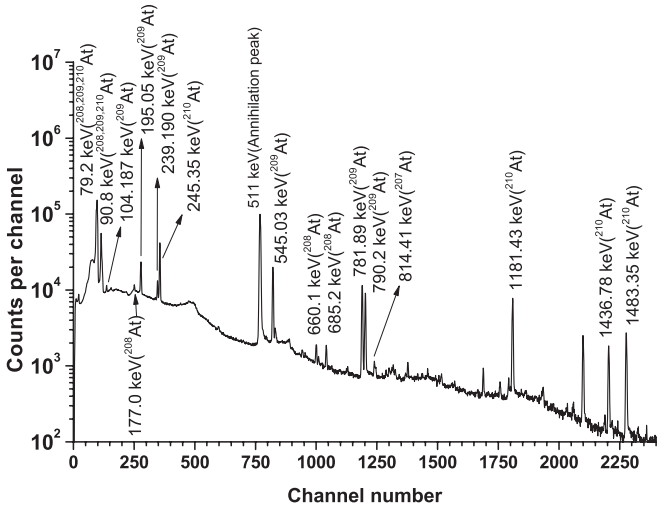

FIG. 1. γ-ray spectrum of the radionuclides produced in ^{7}Li + ^{nat}Pb reaction at 46 MeV incident energy after 1.5 h of EOB.

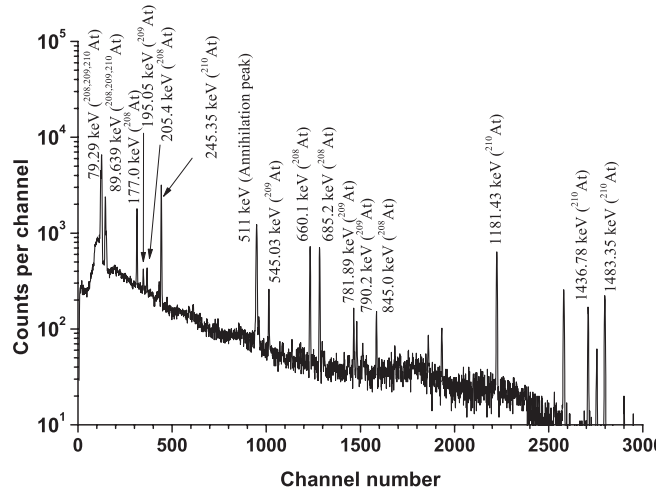

FIG. 2. γ-ray spectrum of the radionuclides produced in ^{9}Be + ^{nat}Tl reaction at 47.6 MeV incident energy after 2 h of EOB.

area associated with a particular γ-ray energy. The nuclear spectroscopic data of the radionuclides studied in this Brief Report are shown in Table I of Ref. [18]. The cross sections of the evaporation residues produced at various incident energies were calculated from the standard activation equation. The total associated error related to the cross-section measurement was determined by including all the probable uncertainties, and the data are presented at the 95% confidence level. A detailed description of the calculation is available elsewhere [19,20].

To compare the measured cross sections, theoretical cross sections of $^{207-210}$At were calculated from ^{7}Li + ^{nat}Pb and ^{9}Be + ^{nat}Tl reactions using the nuclear reaction model codes PACE4 [16] and ALICE91 [14,15].

PACE4 [16] is the modified version of PACE (Projection Angular momentum Coupled Evaporation [21]), working in the framework of LISE++ [22] with several new features. It uses the Hauser-Feshbach model to follow the deexcitation of the excited nuclei. The transmission coefficients for light particle emission were determined from the optical model potential with default optical model parameters. The code internally chooses the level densities and masses it needs during deexcitation. The Gilbert-Cameron level density prescription is used in the present work with level density parameter a equal to A/9 MeV^{-1}. The ratio of a_f/a_n is chosen as unity. Fission is considered as a decay mode using the finite-range fission barriers of Sierk [23]. The compound nuclear fusion cross section is determined using the Bass method [24]. The yrast parameter is taken as unity.

The excitation functions of $^{207-210}$At were calculated using the code ALICE91 [14,15] with the geometry-dependent hybrid model [15] for preequilibrium emissions and the Weisskopf-Ewing formalism for equilibrium emissions. A separate calculation was also performed using ALICE91 with only the Weisskopf-Ewing model option for the excitation functions of $^{208-211}$At. The details of the hybrid model are available in our previous papers [13,25]. The emission of light particles, n, p, d, and α, is considered from the suite of residual nuclides 12 mass units wide and 10 charge units deep including the composite nucleus. The Fermi gas level density was used for the calculation of reaction cross sections. Inverse channel reaction cross sections were calculated using the optical model. The initial exciton number for the preequilibrium emission calculation was chosen to be the number of nucleons in the projectile.

Formation cross sections of the residues were calculated separately from ^{7}Li- and ^{9}Be-induced reactions on each naturally occurring isotope of Pb and Tl, respectively, and the total formation cross section was calculated by taking the weighted average of all the naturally occurring isotopes.

TABLE I. Nuclear spectrometric data [18] of the radionuclides produced through different nuclear reactions.

Isotope	$T_{1/2}$ (h)	Decay mode (%)	E_γ (keV) (I_γ%)	^{7}Li + ^{nat}Pb	E_{th} (MeV)	^{9}Be + ^{nat}Tl	E_{th} (MeV)
^{210}At	8.1	ϵ(99.82)α(0.18)	1181.43(99)	^{208}Pb(^{7}Li,5n)	36.41	^{203}Tl(^{9}Be,2n)	19.41
				^{207}Pb(^{7}Li,4n)	28.80	^{205}Tl(^{9}Be,4n)	34.23
				^{206}Pb(^{7}Li,3n)	21.84		
^{209}At	5.41	ϵ(95.9)α(4.1)	545.03(91)	^{207}Pb(^{7}Li,5n)	36.21	^{203}Tl(^{9}Be,3n)	26.89
				^{206}Pb(^{7}Li,4n)	29.25	^{205}Tl(^{9}Be,5n)	41.71
				^{204}Pb(^{7}Li,2n)	13.93		
^{208}At	1.63	ϵ(99.45)α(0.55)	660.04(89)	^{206}Pb(^{7}Li,5n)	37.99	^{203}Tl(^{9}Be,4n)	35.73
				^{204}Pb(^{7}Li,3n)	22.68		
^{207}At	1.81	ϵ(91.4)α(8.6)	814.41(45)	^{204}Pb(^{7}Li,4n)	30.25		

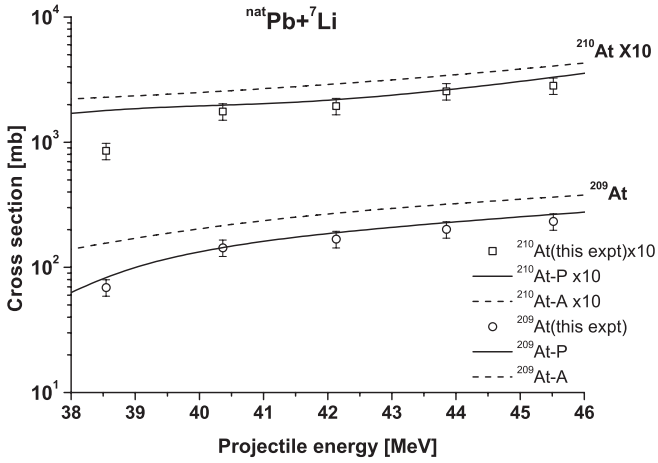

FIG. 3. Comparison between measured cross sections of ^{210}At and ^{209}At from ^{7}Li + ^{nat}Pb reactions and that theoretically predicted from PACE4 and ALICE91. P, PACE4; A, ALICE91.

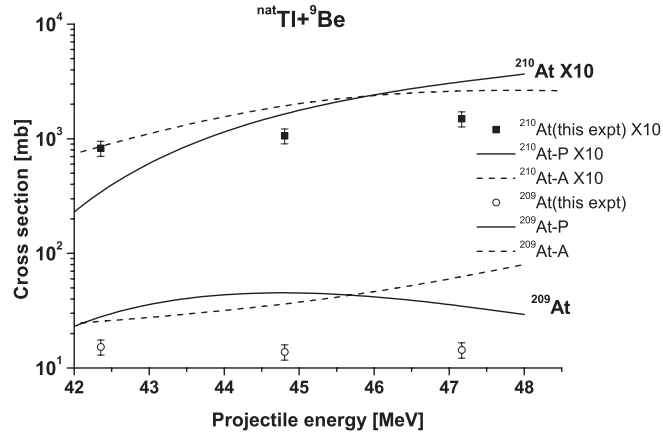

FIG. 5. Same as Fig. 3 for ^{210}At and ^{209}At from ^{9}Be + ^{nat}Tl reaction.

In the following we present the results and discussion of γ-spectra collected at different time intervals after EOB optimized the sensitivity for the detection of the various proton-rich astatine radionuclides. Figures 1 and 2 present γ spectra of the ^{7}Li- and ^{9}Be-irradiated ^{nat}Pb and ^{nat}Tl targets at the highest incident energies, 46 and 47.6 MeV, respectively. The astatine radionuclides produced in the particular target-projectile combination are listed in Table I along with the reaction threshold values. The theoretical investigation [13] predicted the production of ^{211}At (≈400 mb) in the ^{7}Li-induced reaction on ^{nat}Pb. However, it was not possible to identify ^{211}At by γ-ray spectrometry in the present experiment because of its low-intensity γ-ray emissions.

Cross sections measured for $^{207-210}$At from the ^{7}Li + ^{nat}Pb reaction in the 46–38-MeV projectile energy interval and $^{208-210}$At from the ^{9}Be + ^{nat}Tl reaction in the 47.2–42-MeV energy interval are tabulated in Table II and are compared with theoretical predictions of PACE4 and ALICE91 as shown in Figs. 3–6. Although ALICE91 includes preequilibrium emissions, it was observed in general that the preequilibrium contribution is insignificant even for the highest projectile energy we studied. As a result, the comparison is only between the two compound nuclear reaction models, Weisskopf-Ewing and Hauser-Feshbach.

As seen in Fig. 3 the experimental production of ^{210}At and ^{209}At are well reproduced by PACE4, whereas ALICE91 overpredicts the data by ≈40%. Both of the theoretical predictions agree with the measured cross sections for ^{207}At but reproduce neither the measured cross section nor the trend for ^{208}At (Fig. 4). Similar phenomena were observed for the ^{9}Be + ^{nat}Tl reaction (Figs. 5 and 6). The PACE4 calculation underpredicts the measured data at the lowest incident energy whereas it overpredicts the measured data at higher energies for ^{210}At and ^{208}At. ALICE91 also overpredicts the measured data at higher energies but agrees well with the cross-section values at 42.3 MeV for ^{210}At and ^{208}At, respectively. However, no agreement was found between theory and experiment for ^{209}At, and the measured cross sections of ^{209}At are almost constant in the 42–47.5-MeV projectile energy range. It is difficult to make any definite comments on the cross-section data because only a small incident energy range was studied in this Brief Report. However, analysis of the measured data reveals a characteristic signature of a compound nuclear reaction producing $^{207-210}$At in the reported incident energy region. It was observed

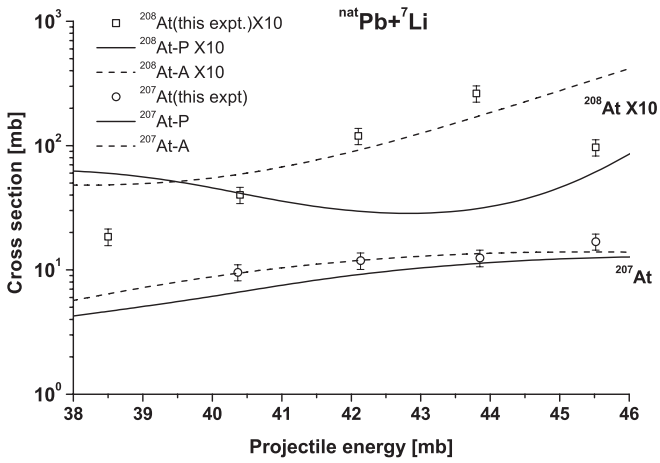

FIG. 4. Same as Fig. 3 for ^{208}At and ^{207}At.

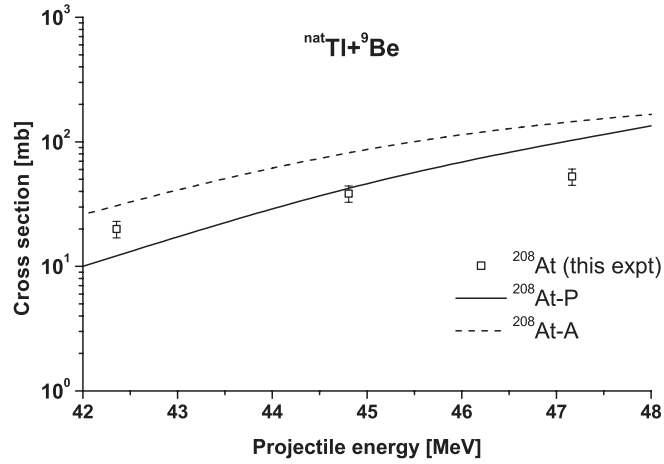

FIG. 6. Same as Fig. 5 for ^{208}At.

TABLE II. Cross section of At radionuclides produced in ^{7}Li + ^{nat}Pb and ^{9}Be + ^{nat}Tl reactions.

E (MeV)	^{7}Li + ^{nat}Pb: σ (mb)				E (MeV)	^{9}Be + ^{nat}Tl: σ (mb)		
	^{210}At	^{209}At	^{208}At	^{207}At		^{210}At	^{209}At	^{208}At
38.5	85.2 ± 12.8	69.1 ± 10.4	1.9 ± 0.3		42.4	82.7 ± 12.4	15.3 ± 2.3	19.9 ± 3.0
40.4	176.0 ± 26.4	143.6 ± 21.5	4.0 ± 0.6	9.6 ± 1.4	44.8	106.0 ± 15.9	13.8 ± 2.1	38.5 ± 5.8
42.1	194.5 ± 29.2	168.5 ± 25.3	12.0 ± 1.8	11.9 ± 1.8	47.2	149.4 ± 22.4	14.4 ± 2.2	52.7 ± 7.9
43.8	255.1 ± 38.3	201.4 ± 30.2	26.3 ± 3.9	12.5 ± 1.9				
45.5	283.0 ± 42.4	232.4 ± 34.9	9.7 ± 1.5	16.9 ± 2.5				

experimentally that the production of ^{208}At is higher than that of ^{209}At in this energy range. This fact is in agreement with the theoretical evaluation. Others have observed that the Weisskopf-Ewing model, owing to limitations of the underlying physics, gives higher cross-section values than the more rigorous Hauser-Feshbach model. This fact is also reflected in the comparison shown in the figures.

In conclusion, this Brief Report gives the measured production cross sections of ^{207,208,209,210}At from two separate heavy-ion-induced reactions, ^{7}Li + ^{nat}Pb and ^{9}Be + ^{nat}Tl, respectively. Production cross sections of the astatine radionuclides, which are expected to be evaporation residues, were compared with two established evaporation models: Weisskopf-Ewing and Hauser-Feshbach. Measured cross sections are in general lower than the theoretical expectations. The present work is limited because of the available projectile energy and reports only a small part of the total excitation functions possible for these evaporation residues. However, the measured cross-section data are important to validate the theoretical predictions reported in Ref. [13] and to enrich the nuclear reaction data bank toward the production of various proton-rich astatine radionuclides.

The authors are thankful to the target laboratory of the Variable Energy Cyclotron Centre, Kolkata, India, for preparing targets. Thanks to Pelletron staff of the BARC-TIFR Pelletron Facility, Mumbai, for their cooperation and help during the experiment. M. Maiti is thankful to the Council of Scientific and Industrial Research (CSIR) for providing necessary grants. This work was carried out as part of the SINP-DAE, XI five-year plan project Trace Analysis: Detection, Dynamics and Speciation (TADDS).

[1] A. Hermanne, F. Trknyi, S. Takcs, Z. Szucs, Yu. N. Shubin, and A. I. Dityuk, Appl. Radiat. Isotopes **63**, 1 (2005).
[2] G. Henriksen, S. Messelt, E. Olsen, and R. H. Larsen, Appl. Radiat. Isotopes **54**, 839 (2001).
[3] M. K. Schultz, M. Hammond, J. T. Cessna, P. Plascjak, B. Norman, L. Szajek, K. Garmestani, B. E. Zimmerman, and M. Unterweger, Appl. Radiat. Isotopes **64**, 1365 (2006).
[4] F. Groppi, M. L. Bonardi, C. Birattari, E. Menapace, K. Abbas, U. Holzwarth, A. Alfarano, S. Morzenti, C. Zona, and Z. B. Alfassi, Appl. Radiat. Isotopes **63**, 621 (2005).
[5] Z. Szucs, F. Szelecsenyi, J. Bergmann, S. J. Heselius, and O. Solin, Radiochim. Acta **65**, 87 (1994).
[6] O. N. Vysotsky, A. V. Gonchar, G. N. Kozeratskaya, S. N. Kondratiev, V. D. Sklyarenko, and V. V. Tokarevsky, Izv. Ross. Akad. Nauk, Ser. Fiz. **56**, 102 (1992).
[7] Y. Nagame, Y. Nakamura, M. Takahashi, K. Sueki, and H. Nakahara, Nucl. Phys. A **486**, 77 (1988).
[8] Y. W. Wu, Z. H. Liu, C. J. Lin, H. Q. Zhang, M. Ruan, F. Yang, Z. C. Li, M. Trotta, and K. Hagino, Phys. Rev. C **68**, 044605 (2003).
[9] A. A. Hassan *et al.*, Izv. Ross. Akad. Nauk, Ser. Fiz. **70**, 1558 (2006).
[10] K. Roy and S. Lahiri, Appl. Radiat. Isotopes **66**, 571 (2008).
[11] S. Lahiri, K. Roy, and S. Sen, Appl. Radiat. Isotopes **66**, 1901 (2008).
[12] M. Maiti and S. Lahiri, J. Radioanal. Nucl. Chem. **281**, 501 (2009).
[13] M. Maiti and S. Lahiri, Phys Rev. C **79**, 024611 (2009).
[14] M. Blann, Lawrence Livermore National Laboratory Report No. UCID 19614, 1982 (unpublished); International Centre for Theoretical Physics Workshop on Applied Nuclear Theory and Nuclear Model Calculations for Nuclear Technology Applications, Trieste, Italy, SMR/284-1, 1988 (unpublished).
[15] M. Blann and H. K. Vonach, Phys. Rev. C **28**, 1475 (1983).
[16] [http://groups.nscl.msu.edu/lise/5_13/lise_5_13.html].
[17] J. F. Ziegler, J. P. Biersack, and U. Littmark, *The Stopping and Range of Ions in Solids* (Pergamon Press, New York, 1985).
[18] [http://www.nndc.bnl.gov/nudat2/].
[19] M. Maiti and S. Lahiri, Phys Rev. C **81**, 024603 (2010).
[20] M. Maiti, Phys Rev. C **84**, 044615 (2011).
[21] A. Gavron, Phys. Rev. C **21**, 230 (1980).
[22] O. B. Tarasov and D. Bazin, Nucl. Instrum. Methods **204**, 174 (2003).
[23] A. J. Sierk, Phys. Rev. C **33**, 2039 (1986).
[24] R. Bass, Phys. Rev. Lett. **39**, 265 (1977).
[25] M. Maiti, S. N. Roy, M. Nandy, and P. K. Sarkar, Phys. Rev. C **71**, 034601 (2005).